SLAC-PUB-16913

New Insights into Color Confinement, Hadron Dynamics, Spectroscopy, and Jet Hadronization from Light-Front Holography and Superconformal Algebra

Stanley J. Brodsky

SLAC National Accelerator Laboratory, Stanford University [1]

Abstract

A fundamental problem in hadron physics is to obtain a relativistic color-confining, first approximation to QCD which can predict both hadron spectroscopy and the frame-independent light-front wavefunctions underlying hadron dynamics. The QCD Lagrangian with zero quark mass has no explicit mass scale; the classical theory is conformally invariant. Thus a fundamental problem is understand how the mass gap, and ratios of masses such as m_ρ/m_p—- can arise in chiral QCD. de Alfaro, Fubini, and Furlan have made an important observation that a mass scale can appear in the equations of motion without affecting the conformal invariance of the action if one adds a term to the Hamiltonian proportional to the dilatation operator or the special conformal operator and rescales the time variable. If one applies the same procedure to the light-front Hamiltonian, it leads uniquely to a confinement potential $\kappa^4\zeta^2$ for mesons, where ζ^2 is the LF radial variable conjugate to the $q\bar{q}$ invariant mass squared. The same result, including spin terms, is obtained using light-front holography – the duality between light-front dynamics and AdS_5, the space of isometries of the conformal group – if one modifies the action of AdS_5 by the dilaton $e^{\kappa^2 z^2}$ in the fifth dimension z. When one generalizes this procedure using superconformal algebra, the resulting light-front eigensolutions predict a unified Regge spectroscopy of meson, baryon, and tetraquarks, including remarkable supersymmetric relations between the masses of mesons and baryons of the same parity. One also predicts observables such as hadron structure functions, transverse momentum distributions, and the distribution amplitudes defined from the hadronic light-front wavefunctions. The mass scale κ underlying confinement and hadron masses can be connected to the parameter $\Lambda_{\overline{MS}}$ in the QCD running coupling by matching the nonperturbative dynamics to the perturbative

[1] Invited seminar presented at Tomsk National University (via SKYPE), June 7, 2016

sjbth@slac.stanford.edu

This material is based upon work supported by the U.S. Department of Energy, Office of Science, under Contract No. DE-AC02-76SF00515.

QCD regime. The result is an effective coupling $\alpha_s(Q^2)$ defined at all momenta. The matching of the high and low momentum transfer regimes also determines a scale Q_0 which sets the interface between perturbative and nonperturbative hadron dynamics. The use of Q_0 to resolve the factorization scale uncertainty for structure functions and distribution amplitudes, in combination with the principle of maximal conformality (PMC) for setting the renormalization scales without scheme-independence, can greatly improve the precision of perturbative QCD predictions for collider phenomenology. Even though many quarks and gluons are produced in intermediate states in a high energy collision, only hadrons appear in the final on-shell final state due to color confinement. AdS/QCD also gives insight into the hadronization of jets into the observed final states at the amplitude level.. The absence of vacuum excitations of the causal, frame-independent front-form vacuum also has important consequences for the cosmological constant.

Contents

1 Introduction

One of the most elegant features of quantum field theory is supersymmetry – a theory where the fermionic and bosonic eigensolutions have the same mass. As I will discuss here, the observed hadronic spectrum of $SU(3)_C$ QCD exhibits the supersymmetric features predicted by superconformal algebra. The phenomenological Regge trajectories $M_h^2 \propto L_H$ for both mesons and baryons are observed to have parallel slopes despite the fact that baryons are bound states of three quarks. Remarkably supersymmetry predicts that the observed hadronic masses match when one compares mesons with orbital angular momentum L_M with baryons with orbital angular momentum $L_B = L_M - 1$. This is illustrated for ρ and Δ trajectories in Fig. 1. The matching states also have matching twist $2 + L_M = 3 + L_B$. As we shall see, these phenomena are predicted by superconformal algebra and light-front holography.

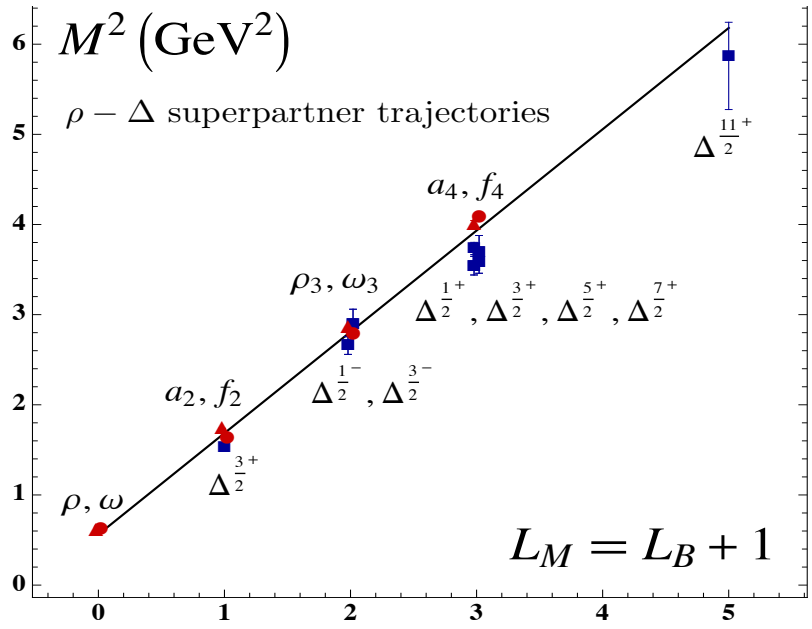

Figure 1: Comparison of the ρ/ω meson Regge trajectory with the $J = 3/2$ Δ baryon trajectory. Superconformal algebra predicts the degeneracy of the meson and baryon trajectories if one identifies a meson with internal orbital angular momentum L_M with its superpartner baryon with $L_M = L_B + 1$. See Refs. [1, 2].

A fundamental problem in hadron physics is to obtain a color-confining first approximation to QCD which can predict both the hadron spectrum and the LFWFs underlying hadron phenomenology. The QCD Lagrangian with zero quark mass has no explicit mass scale; the classical theory is conformally invariant. A profound question is then to understand how the proton mass and other hadronic mass scales – the mass gap – can arise even when $m_q = 0$. In fact, chiral QCD has no knowledge of units such as MeV. However, a remarkable principle, first demonstrated by de Alfaro, Fubini and Furlan (dAFF) [3] in $1+1$ quantum mechanics, is that a mass scale can appear in a Hamiltonian without affecting the conformal invariance of the action. The essential step of DAFF is to add to the conformal Hamiltonian H_0 terms proportional to the dilation operator D and the special conformal operator K. The coefficients introduce the mass scale κ, and the result is $H = H_0 + V$, where V a harmonic oscillator potential $V(x) = \kappa^2 x^2$. The action remains conformal when one changes to a new time variable. De Téramond, Dosch, and I [4] have shown that a mass gap and a fundamental color confinement scale appear when one extends the dAFF procedure to light-front Hamiltonian theory.

The conformal group has an elegant 2×2 Pauli matrix representation called superconformal algebra, originally discovered by Haag, Lopuszanski, and Sohnius [5]. The conformal Hamiltonian operator and the special conformal operators can be represented as anticommutators of Pauli matrices $H = 1/2[Q, Q^\dagger]$ and $K = 1/2[S, S^\dagger]$. As shown by Fubini and Rabinovici, [6], a nonconformal Hamiltonian with a mass scale and universal confinement can then be obtained by shifting $Q \to Q + \omega K$, the analog of the dAFF procedure. In effect one has generalized supercharges of the superconformal algebra [6]. Thus the conformal algebra can be extended even though ω has dimension of mass. The result of this shift of the Hamiltonian is a color-confining harmonic potential in the equations of motion. Remarkably the action remains conformally invariant, and only one mass parameter appears.

As shown by Guy de Téramond, Günter Dosch and myself, the bound-state equations of superconformal algebra are, in fact, Lorentz invariant, frame-independent, relativistic light-front Schrodinger equations and the resulting eigensolutions are the eigenstates of a light-front Hamiltonian obtained from AdS_5 and light-front holography. Light-front quantization at fixed light-front time $\tau = t + z/c$ provides a physical, frame-independent formalism for hadron dynamics and structure. When one makes a measurement such as in deep inelastic lepton-proton scattering $\ell p \to \ell' X$, the hadron is observed along a light-front (LF) – in analogy to a flash photograph – not at a fixed time t. This is the

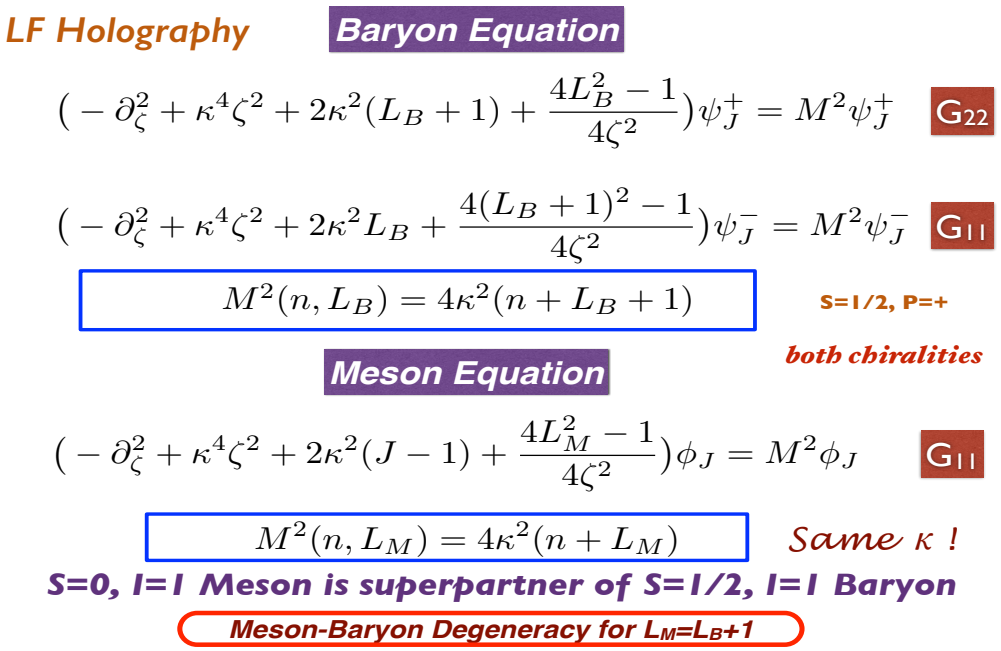

Figure 2: The LF Schrödinger equations for baryons and mesons for zero quark mass derived from the Pauli 2×2 matrix representation of superconformal algebra. The $\psi^\pm$ are the baryon quark-diquark LFWFs where the quark spin $S_q^z = \pm 1/2$ is parallel or antiparallel to the baryon spin $J^z = \pm 1/2$. The meson and baryon equations are identical if one identifies a meson with internal orbital angular momentum L_M with its superpartner baryon with $L_B = L_M - 1$. See Refs. [1, 2, 8].

underlying principle of Dirac's "front form" [7].

Superconformal algebra leads to effective QCD light-front bound-state equations for both mesons and baryons [1, 2, 8]. The resulting set of bound-state equations for confined quarks are shown in Fig. 2. The supercharges connect the baryon and meson spectra and their Regge trajectories to each other in a remarkable manner: the superconformal algebra predicts that the bosonic meson and fermionic baryon masses are equal if one identifies each meson with internal orbital angular momentum L_M with its superpartner baryon with $L_B = L_M - 1$; the meson and baryon superpartners then have the same parity, Since $2+L_M = 3+L_B$, the twist dimension of the meson and baryon superpartners are also the same. As I mentioned before, the comparison between the meson and baryon masses of the ρ/ω Regge trajectory with the spin-3/2 Δ trajectory is shown in Fig. 1.

The eigensolutions of the supersymmetric conformal algebra have a 2×2 Pauli matrix representation, where the upper-left component corresponds to mesonic $q\bar{q}$ color-singlet bound states, the two off-diagonal eigensolutions $\psi^{\pm}$ correspond to two Fock components of baryonic quark-plus color diquark states with equal weight, where the quark spin is parallel or antiparallel to the baryon spin, respectively, and the fourth component corresponds to diquark anti-diquark (tetraquark) bound states. The resulting frame-independent color-confining bound-state LF eigensolutions can be identified with the hadronic eigenstates of confined quarks for $SU(3)$ color. In effect, two of the quarks of the baryonic color singlet qqq bound state bind to a color $\bar{3}_C$ diquark bound state, which then binds by the same color force to the remaining 3_C quark. As shown by t'Hooft in a string model [9], the Y configuration of three quarks is unstable – and reduces to the quark-diquark configuration. The matching of the meson and baryon spectra is thus due to the fact that the same color-confining potential binds two quarks to a diquarks which binds a quarks to an antiquark.

Note that the same slope controls the Regge trajectories of both mesons and baryons in both the orbital angular momentum L and the principal quantum number n. Only one mass parameter $\kappa = \omega^2$ appears; it sets the confinement scale and the hadron mass scale in the chiral limit, as well as the length scale which underlies hadron structure. We will also use the notation $\lambda = \kappa^2$. In addition to the meson and baryon eigenstates, one also predicts color singlet *tetraquark* diquark-antidiquark bound states with the same mass as the baryon.

The LF Schrödinger Equations for baryons and mesons derived from superconformal algebra are shown in Fig. 2. Thus as explained above, the baryons on the proton (Delta) trajectory are bound states of a quark with color 3_C and scalar (vector) diquark with color $\bar{3}_C$ The proton eigenstate labeled ψ^+ (parallel quark and baryon spins) and ψ^- (anti parallel quark and baryon spins) have equal Fock state probability – a feature of "quark chirality invariance". Predictions for the static properties of the nucleons are discussed in Ref. [10].

Superconformal algebra also predicts that the LFWFs of the superpartners are related, and thus the corresponding elastic and transition form factors are related. The resulting predictions meson and baryon timelike form factors can be tested in $e^+e^- \to H\bar{H}'$ reactions.

As illustrated in Fig. 3, the hadronic eigensolutions of the superconformal algebra are themselves 2×2 matrices connected internally by the supersymmetric algebra operators. One can generalize these results to heavy-light $[\bar{Q}q]$ mesons and $[Q[qq]]$ baryons [11]. The

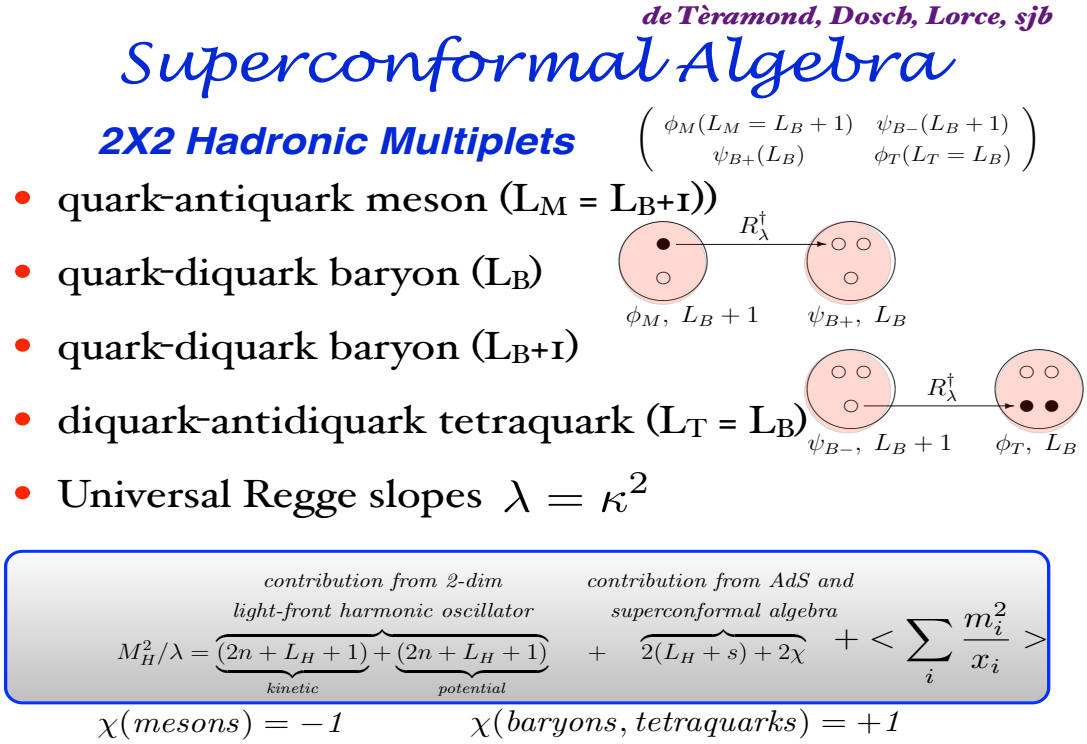

Figure 3: The eigenstates of superconformal algebra have a 2×2 representation of mass degenerate bosons and fermions: a meson with $L_M = L_B + 1$, a baryon doublet with $L_B, L_B + 1$ components and a tetraquark with $L_T = L_B$. The breakdown of LF kinetic, potential, spin, and quark mass contributions to each hadron is also shown. The virial theorem predicts the equality of the LF kinetic and potential contributions.

Regge slopes is found to increase for heavy m_Q as expected from heavy quark effective field theory; however, the supersymmetric connections between the heavy-light hadrons is predicted to be maintained.

2 Light-Front Physics

Measurements of hadron structure such as deep inelastic lepton-proton scattering are made at fixed light-front time $\tau = t + z/c$, like a flash photograph not at a single "instant time". As shown by Dirac [7], boosts are kinematical in the "front form". Thus the front form can be formulated so it is independent of the observer's motion [12] .

The eigenfunctions of the light-front Hamiltonian $H_{LF} = P^+P^- - \vec{P}_\perp^2$ derived from the QCD Lagrangian represents the hadronic mass spectrum, for both individual hadrons and multi-hadrons continuum eigenstates. The eigenvalues of the LF Hamiltonian are the squares of the hadron masses M_H^2: $H_{LF}|\Psi_H >= M_H^2|\Psi_H >$ [12]. Here $P^- = i\frac{d}{d\tau}$ is the LF time evolution operator, and $P^+ = P^0 + P^z$ and $\vec{P}_\perp$ are kinematical. The eigenfunctions of H_{LF} provide hadronic LF Fock state wavefunctions (LFWFs): $\psi_n^H(x_i, \vec{k}_{\perp i}, \lambda_i) =< n|\Psi_H >$, the projection of the hadronic eigenstate on the free Fock basis. The constituents' physical momenta are $p_i^+ = x_i P^+$, and $\vec{p}_{\perp i} = x_i \vec{P}_\perp + \vec{k}_{\perp i}$, and the λ_i label the spin projections S_i^z.

The LFWFs are Poincare' invariant: they are independent of P^+ and $P_\perp$ and are thus independent of the motion of the observer. Since the LFWFs are independent of the hadron's momentum, there is no length contraction [13, 14]. Structure functions are essentially the absolute square of the LFWFs. One thus measures the same structure function in an electron-ion collider as in an electron-scattering experiment where the target hadron is at rest.

Light-front wavefunctions thus provide a direct link between the QCD Lagrangian and hadron structure. Since they are defined at a fixed τ, they connect the physical on-shell hadronic state to its quark and gluon parton constituents, not at off-shell energy, but off-shell in invariant mass squared $\mathcal{M}^2 = (\sum_i k_i^\mu)^2$. They thus control the transformation of the quarks and gluons in an off-shell intermediate state into the observed final on-shell hadronic state. See Fig. 4.

The LFWFs thus play the same role in hadron physics as the Schrödinger wavefunctions which encode the structure of atoms in QED. The elastic and transition form factors of hadrons, weak-decay amplitudes and distribution amplitudes are overlaps of LFWFs; structure functions, transverse momentum distributions and other inclusive

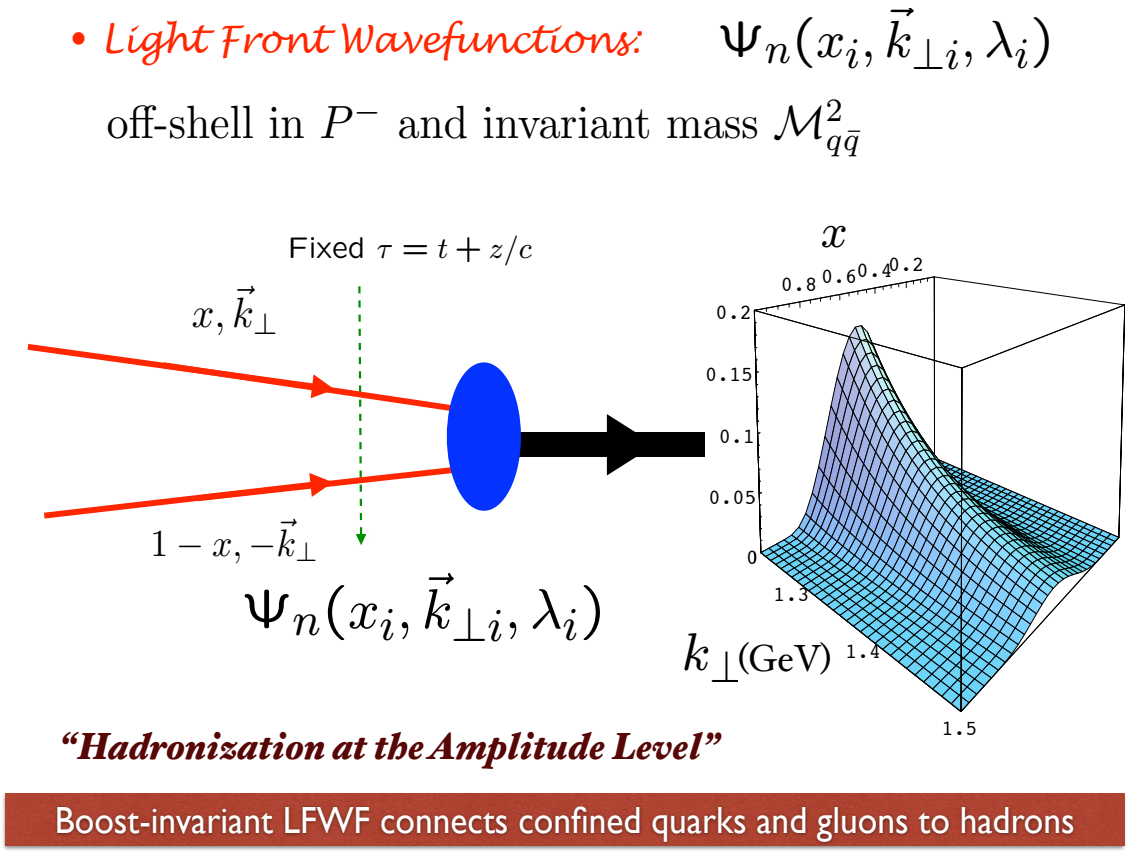

Figure 4: The meson LFWF connects the intermediate $q\bar{q}$ state, which is off the P^- energy shell and thus off-the-invariant mass shell $\mathcal{M}^2 > m_H^2$ to the physical meson state with $\mathcal{M}^2 = m_H^2$. The q and $\bar{q}$ can be regarded as effective dressed fields

.

observables are constructed from the squares of the LFWFs. In contrast one cannot compute form factors of hadrons or other current matrixelements of hadrons from overlap of the usual "instant" form wavefunctions since one must also include contributions where the photon interacts with connected but acausal vacuum-induced currents. The calculation of deeply virtual Compton scattering using LFWFs is given in Ref. [15]. One can also compute the gravitational form factors of hadrons. In particular, one can show that the anomalous gravitomagnetic moment $B(q^2 = 0)$ vanishes identically for any LF Fock state [16], in agreement with the equivalence theorem of gravity [17, 18].

The hadronic LFWFs predicted by light-front holography and superconformal algebra are functions of the LF kinetic energy $\vec{k}_\perp^2/x(1-x)$ – the conjugate of the LF radial variable $\zeta^2 = b_\perp^2 x(1-x)$ – times a function of $x(1-x)$; they do not factorize as a function of $\vec{k}_\perp^2$ times a function of x. The resulting nonperturbative pion distribution amplitude $\phi_\pi(x) = \int d^2\vec{k}_\perp \psi_\pi(x, \vec{k}_\perp) = (4/\sqrt{3}\pi) f_\pi \sqrt{x(1-x)}$, see Fig. 5, which controls hard exclusive process, is consistent with the Belle data for the photon-to-pion transition form factor [19]. The AdS/QCD light-front holographic eigenfunction for the ρ meson LFWF $\psi_\rho(x, \vec{k}_\perp)$ gives excellent predictions for the observed features of diffractive ρ electroproduction $\gamma^* p \to \rho p'$, as shown by Forshaw and Sandapen [20]

3 Light-Front Holography

Five-dimensional AdS_5 space provides a geometrical representation of the conformal group. The color-confining light-front equation for mesons of arbitrary spin J can be derived [21] from the holographic mapping of the "soft-wall model" modification of AdS_5 space for the specific dilaton profile $e^{+\kappa^2 z^2}$, where one identifies the fifth dimension coordinate z with the light-front coordinate ζ. Remarkably , AdS_5 is holographically dual to $3+1$ spacetime at fixed light-front time $\tau = t + z/c$. The holographic dictionary is summarized in Fig. 6 The combination of light-front dynamics, its holographic mapping to AdS_5 space, and the dAFF procedure provides new insight into the physics underlying color confinement, the nonperturbative QCD coupling, and the QCD mass scale. A comprehensive review is given in Ref. [22]. The $q\bar{q}$ mesons and their valence LF wavefunctions are the eigensolutions of the frame-independent relativistic bound state LF Schrödinger equation – the same meson equation that is derived using suoerconformal algebra. The mesonic $q\bar{q}$ bound-state eigenvalues for massless quarks are $M^2(n, L, S) = 4\kappa^2(n + L + S/2)$. The equation predicts that the pion eigenstate $n = L = S = 0$ is massless at zero quark mass. The Regge spectra of the pseudoscalar

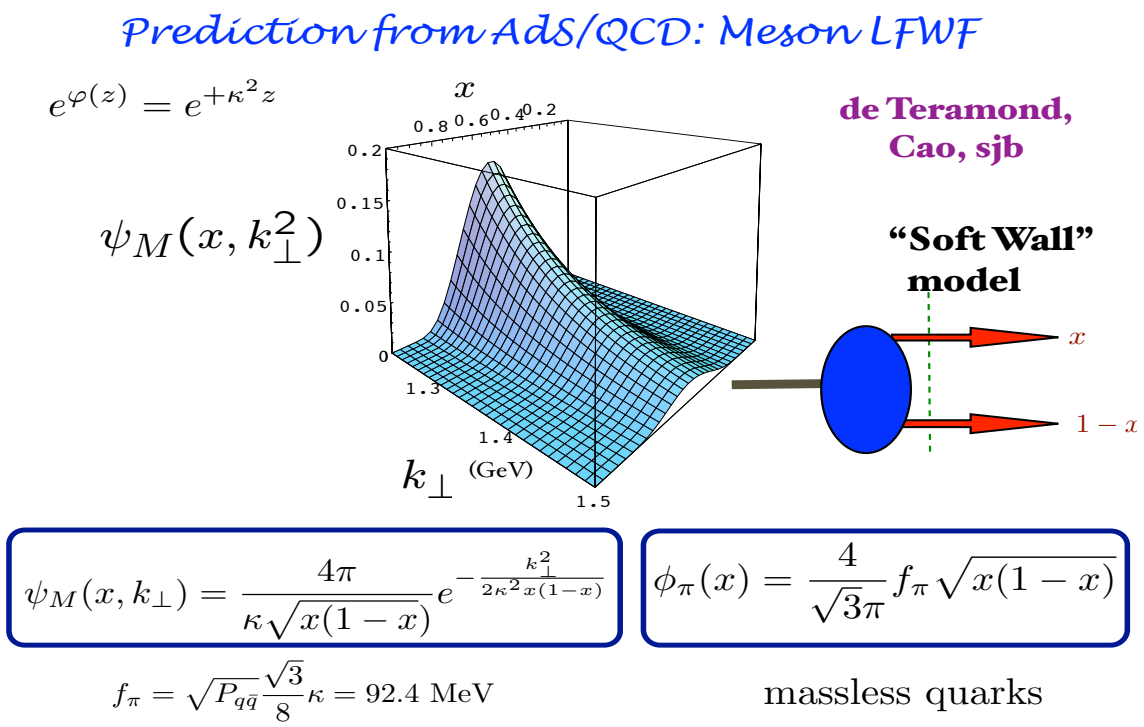

Figure 5: Prediction from AdS/QCD and Light-Front Holography for meson LFWFs $\psi_M(x, \vec{k}_\perp)$ and the pion distribution amplitude.

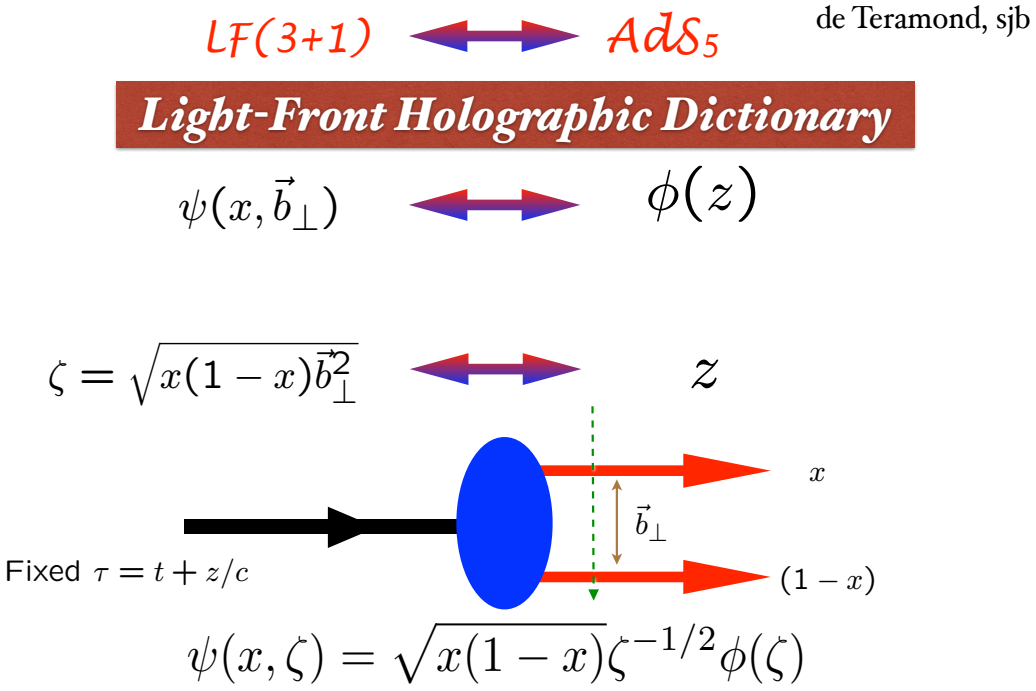

Figure 6: The holographic dictionary which maps the fifth dimension variable z of the five-dimensional AdS_5 space to the LF radial variable ζ where $\zeta^2 = b_\perp^2(1-x)$. The same physics transformation maps the AdS_5 and $(3+1)$ LF expressions for electromagnetic and gravitational form factors to each other. From Ref. [21].

$S = 0$ and vector $S = 1$ mesons are predicted correctly, with equal slope in the principal quantum number n and the internal orbital angular momentum L. A comparison with experiment is shown in Fig. 7.

Light-Front Holography not only predicts meson and baryon spectroscopy successfully, but also hadron dynamics, including vector meson electroproduction, hadronic light-front wavefunctions, distribution amplitudes, form factors, and valence structure functions. The application to the deuteron elastic form factors and structure functions is given in Ref. [23, 24]

4 Color Confinement from LF Holography

Remarkably, the light-front potential using the DAFF procedure has the unique form of a harmonic oscillator $\kappa^4\zeta^2$ in the light-front invariant impact variable ζ where $\zeta^2 = b_\perp^2 x(1-x)$. The result is a single-variable frame-independent relativistic equation of motion for $q\bar{q}$ bound states, a "Light-Front Schrödinger Equation" [25], analogous to the nonrelativistic radial Schrödinger equation in quantum mechanics. The same result, including spin terms, is obtained using light-front holography – the duality between the front form and AdS_5, the space of isometries of the conformal group – if one modifies the action of AdS_5 by the dilaton $e^{\kappa^2 z^2}$ in the fifth dimension z. The Light-Front Schrödinger Equation incorporates color confinement and other essential spectroscopic and dynamical features of hadron physics, including a massless pion for zero quark mass and linear Regge trajectories with the same slope in the radial quantum number n and internal orbital angular momentum L. When one generalizes this procedure using superconformal algebra, the resulting light-front eigensolutions predict a unified Regge spectroscopy of meson, baryon, and tetraquarks, including remarkable supersymmetric relations between the masses of mesons and baryons of the same parity.

It is interesting to note that the contribution of the *'H'* diagram to $Q\bar{Q}$ scattering is IR divergent as the transverse separation between the Q and the $\bar{Q}$ increases [26]. This is a signal that pQCD is inconsistent without color confinement. The sum of such diagrams could sum to the confinement potential $\kappa^4\zeta^2$ dictated by the dAFF principle that the action remains conformally invariant despite the appearance of the mass scale κ in the Hamiltonian. The $\kappa^4\zeta^2$ confinement interaction between a q and $\bar{q}$ will induce a κ^4/s^2 correction to $R_{e^+e^-}$, replacing the $1/s^2$ signal usually attributed to a vacuum gluon condensate.

It should be emphasized that the value of the mass scale κ is not determined ab-

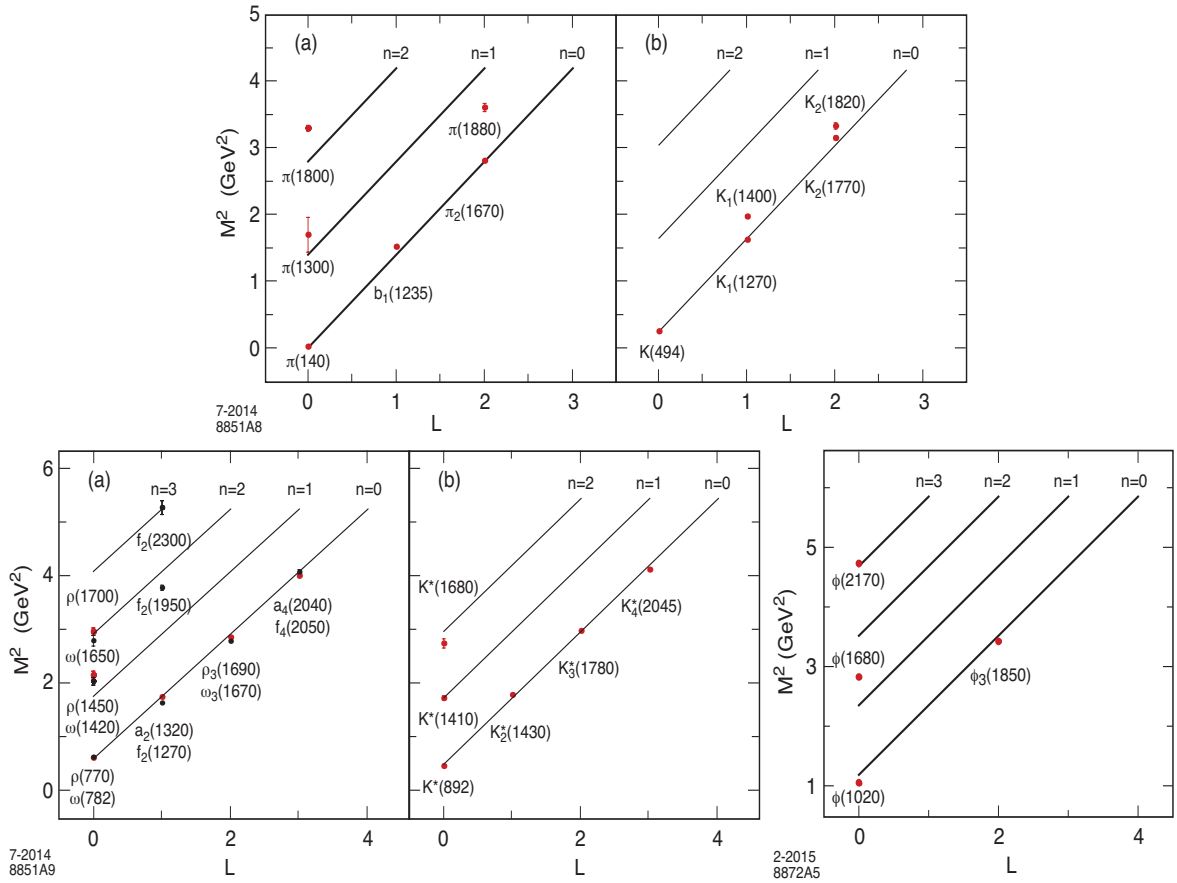

Figure 7: Comparison of the AdS/QCD prediction $M^2(n, L, S) = 4\kappa^2(n + L + S/2)$ for the orbital L and radial n excitations of the meson spectrum with experiment. The pion is predicted to be massless for zero quark mass. The u, d, s quark masses can be taken into account by perturbing in $< m_q^2/x >$. The fitted value of $\kappa = 0.59$ MeV for pseudoscalar mesons, and $\kappa = 0.54$ MeV for vector mesons.

solutely by QCD. Only ratios of masses are determined, and the theory has dilation invariance under $\kappa \to C\kappa$, In a sense, chiral QCD has an "extended conformal invariance." The resulting new time variable which retains the conformal invariance of the action, has finite support, conforming to the fact that the LF time between the interactions with the confined constituents is finite.

The finite time difference $\Delta\tau$ between the LF times τ of the quark constituents of the proton could be measured using positronium-proton scattering $[e^+e^-]p \to e^+e^-p'$. This process, which measures double diffractive deeply virtual Compton scattering for two spacelike photons, is illustrated in Fig. 8 One can also study the dissociation of relativistic positronium atoms to an electron and positron with light front momentum fractions x and $1-x$ and opposite transverse momenta in analogy to the E791 measurements of the diffractive dissociation of the pion to two jets [27] The LFWF of positronium in the relativistic domain is the central input. One can produce a relativistic positronium beam using the collisions of laser photons with high energy photons or by using Bethe-Heitler pair production below the e^+e^- threshold. The production of parapositronium via the collision of photons is analogous to pion production in two-photon collisions and Higgs production via gluon-gluon fusion.

.

4.1 Light-Front Theory and QCD

One can derive the exact from of the H_{LF} directly from the QCD Lagrangian and avoid ghosts and longitudinal gluonic degrees of freedom by choosing to work in the light-cone gauge $A^+ = 0$. The quark masses appear in the LF kinetic energy as $\sum_i \frac{m^2}{x_i}$. This can be derived from the Higgs theory quantized using LF dynamics. The confined quark field ψ_q couples to the background Higgs field $g_{\overline{\Psi}_q} < H > \Psi_q$ via its Yukawa scalar matrix element coupling $g_q < H > \bar{u}(p)1u(p) = m_q \times \frac{m_q}{x} = \frac{m^2}{x}$.

PQCD factorization theorems and the DGLAP [28, 29, 30] and ERBL [31, 32, 33, 34] evolution equations can also be derived using the light-front Hamiltonian formalism [32]. In the case of an electron-ion collider, one can represent the cross section for $e-p$ colisions as a convolution of the hadron and virtual photon structure functions times the subprocess cross-section in analogy to hadron-hadron colisions. This nonstandard description of $\gamma^* p \to X$ reactions gives new insights into electroproduction physics – physics not apparent in the usual infinite-momentum frame description, such as the dynamics of heavy quark-pair production. Intrinsic heavy quarks at high x also play an important role [35].

The LF Heisenberg equation can in principle be solved numerically by matrix diagonalization using the "Discretized Light-Cone Quantization" (DLCQ) [36] method. Anti-periodic boundary conditions in x^- render the k^+ momenta discrete as well as limiting the size of the Fock basis. In fact, one can easily solve $1+1$ quantum field theories such as QCD$(1+1)$ [37] for any number of colors, flavors and quark masses using DLCQ. Unlike lattice gauge theory, the nonpertubative DLCQ analysis is in Minkowski space, is frame-independent, and is free of fermion-doubling problems. AdS/QCD, based on the AdS_5 representation of the conformal group in five dimensions, maps to physical 3+1 space-time at fixed LF time; this correspondence, "light-front holography" [25], is now providing a color-confining approximation to H_{LF}^{QCD} for QCD(3+1). This method gives a remarkable first approximation to hadron spectroscopy and hadronic LFWFs. A new method for solving nonperturbative QCD "Basis Light-Front Quantization" (BLFQ) [38], uses the eigensolutions of a color-confining approximation to QCD (such as LF holography) as the basis functions, rather than the plane-wave basis used in DLCQ, thus incorporating the full dynamics of QCD. LFWFs can also be determined from the covariant Bethe-Salpeter wavefunction by integrating over k^- [39]. A review of the light-front formalism is given in Ref. [12].

5 Calculations using LF-Time-Ordered Perturbation Theory and Hadronization at the Amplitude Level

LF-time-ordered perturbation theory can be advantageous for perturbative QCD calculations. An excellent example of LF-time-ordered perturbation theory is the computation of multi-gluon scattering amplitudes by Cruz-Santiago and Stasto [42]. In this method, the propagating particles are on their respective mass shells: $k_\mu k^\mu = m^2$, and intermediate states are off-shell in invariant mass; *i.e.*, $P^- \neq \sum k_i^-$. Unlike instant form, where one must sum $n!$ frame-dependent amplitudes, only the τ-ordered diagrams where each propagating particle has positive $k^+ = k^0 + k^z$ can contribute. The number of nonzero amplitudes is also greatly reduced by noting that the total angular momentum projection $J^z = \sum_i^{n-1} L_i^z + \sum_i^n S_i^z$ and the total P^+ are conserved at each vertex. In a renormalizable theory, the change in orbital angular momentum is limited to $\Delta L^z = 0, \pm 1$ at each vertex [43].

A remarkable advantage of LF time-ordered perturbation theory (LFPth) is that the calculation of a subgraph of any order in pQCD only needs to be done once; the result

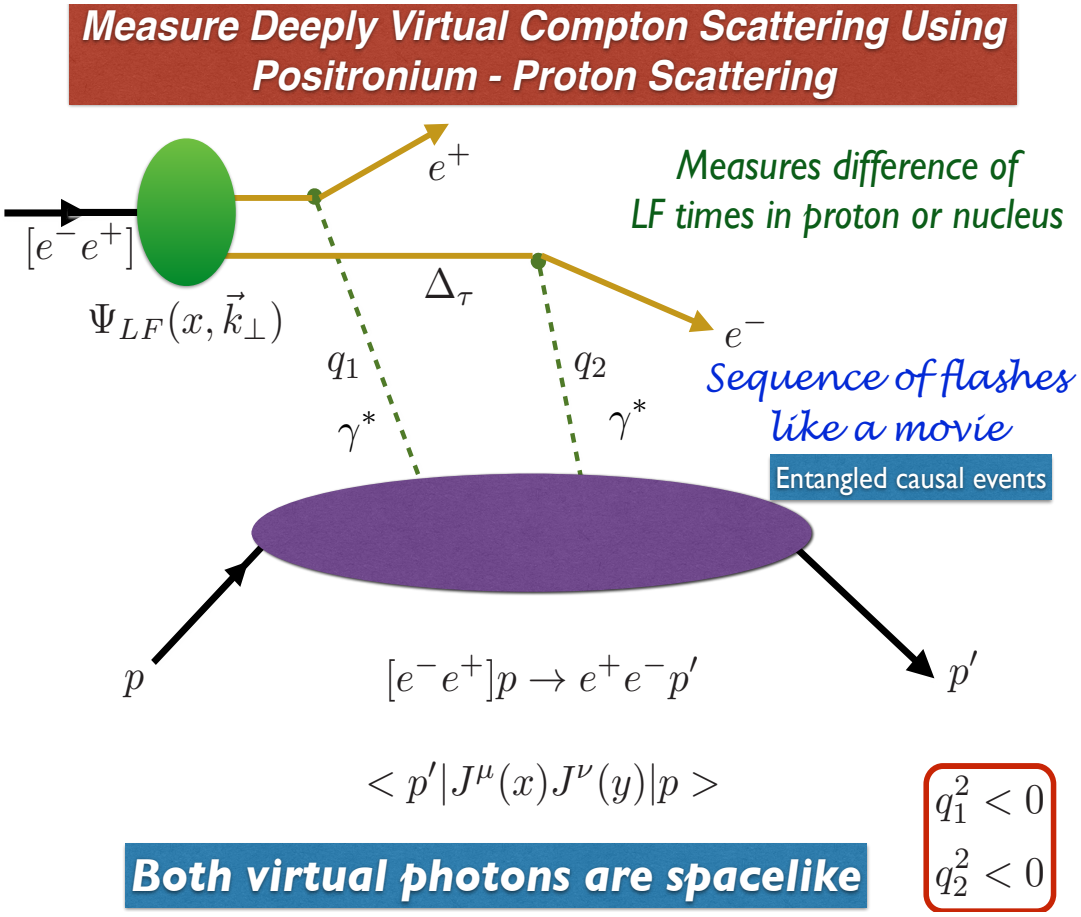

Figure 8: Doubly Virtual Compton scattering on a proton (or nucleus) can be measured for two *spacelike* photons $q_1^2, q_2^2 < 0$ with minimal, tunable, skewness ξ using positronium-proton scattering $[e^+e^-]p \to e^+e^-p'$. One can also measure double deep inelastic scattering and elastic positronium-proton scattering. One can also create a beam of "true muonium" atoms $[\mu^-\mu^-]$ [40, 41] using Bethe-Heitler pair production just below threshold.

can be stored in a "history" file. This is due to the fact that in LFPth the numerator algebra is independent of the process; the denominator changes, but only by a simple shift of the initial P^-. Another simplification is that loop integrations are three dimensional: $\int d^2\vec{k}_\perp \int_0^1 dx$. Unitarity and explicit renormalization can be implemented using the "alternate denominator" method which defines the required subtraction counterterms [44].

The new insights into color confinement given by AdS/QCD suggest that one could compute hadronization at amplitude level [45] using the confinement interaction and the LFWFs predicted by AdS/QCD and Light-Front Holography. For example, as illustrated in Fig. 4, the meson LFWF connects the off-the-invariant mass shell quark and antiquark to the on-shell asymptotic physical meson state.

One can postulate that the invariant mass of a color-singlet cluster $\mathcal{M}$ is the variable which separates perturbative and nonperturbative dynamics. For example, consider e^+e^- annihilation using LF τ - ordered perturbation theory. At an early stage in LF time the annihilation will produce jets of quarks and gluons in an intermediate state that are off the P^- energy shell. If a color-singlet cluster of partons in a jet satisfies $\mathcal{M}^2 - M_H^2 < \kappa^2$, the cluster constituents are effective degrees of freedom will be ruled by the $\kappa^4\zeta^2$ color-confinement potential. At this stage, the LFWF ψ_H converts the off-shell partons to the asymptotic states, the on-shell hadrons. If $\mathcal{M}^2 > \kappa^2$ one can apply pQCD corrections; e.g. from DGLAP and ERBL evolution [31, 32, 33, 34] .

A model for the two stages of hadronization and evolution is illustrated in Fig. 9. In the off-shell domain $\mathcal{M}^2 - M_H^2 > \kappa^2$, the intermediate quarks and gluons obey DGLAP and ERBL evolution.

Thus quarks and gluons can appear in intermediate off-shell states, but only hadrons are produced asymptotically. Thus the AdS/QCD Light-Front Holographic model suggests how one can implement the transition between perturbative and nonperturbative QCD. For a QED analog, see Refs. [40, 41].

6 The Light-Front Vacuum

It is important to distinguish the LF vacuum from the conventional instant-form vacuum. The eigenstates of the instant-form Hamiltonian describe a state defined at a single instant of time t over all space, and they are thus acausal as well as frame-dependent. The instant-form vacuum is defined as the lowest energy eigenstate of the instant-form Hamiltonian. As discussed by Zee [46], the cosmological constant is of

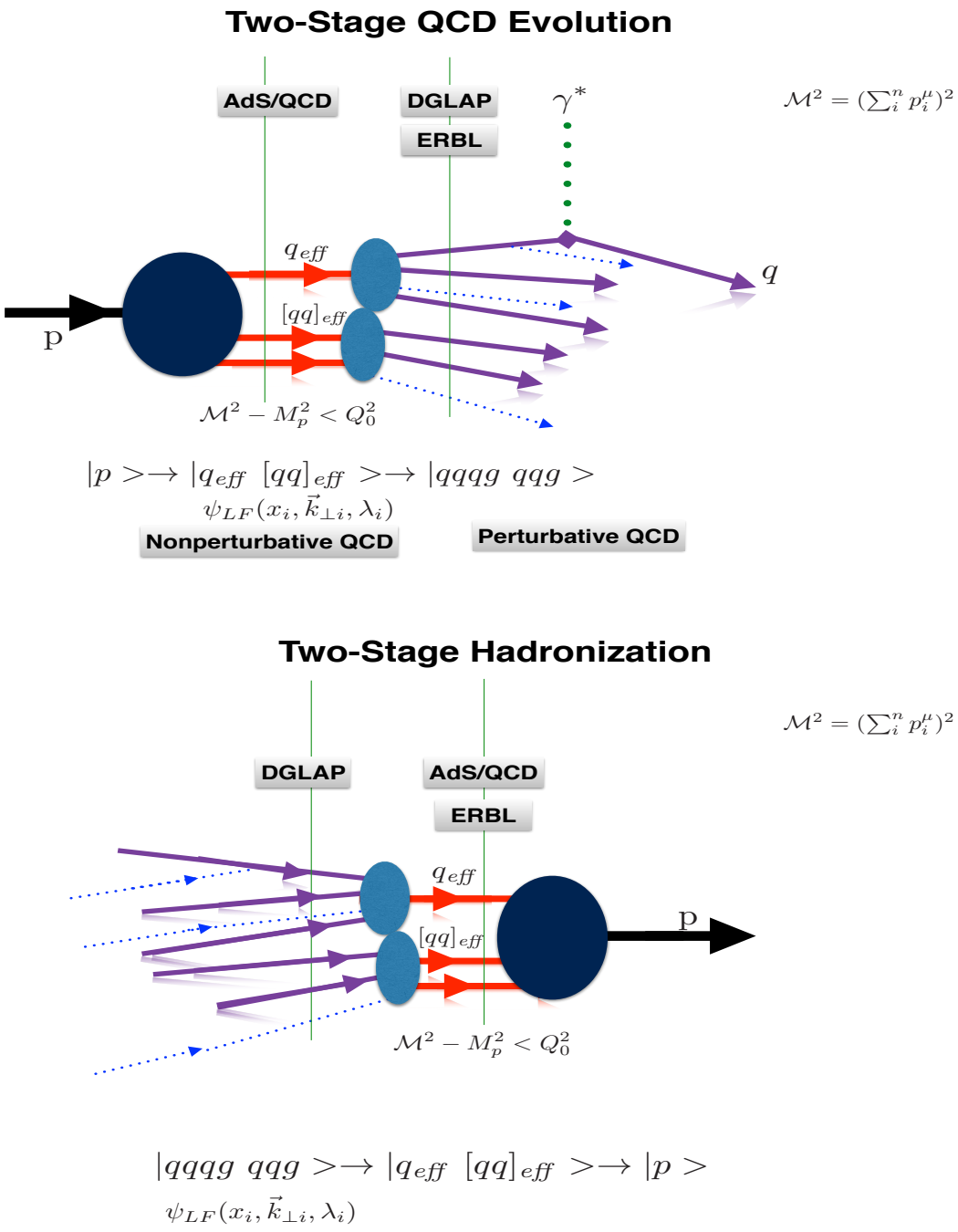

Figure 9: *A*. A model for evolution starting with a nonperturbative hadronic LFWF. *B*. Hadronization and evolution ending with a hadronic LFWF. The intermediate quark and gluon states are off the P^- energy shell and thus off-the-invariant mass shell $\mathcal{M}^2 > m_H^2$ In the off-shell domain $\mathcal{M}^2 - M_H^2 > \kappa^2$, the intermediate quarks and gluons obey the DGLAP and ERBL QCD evolution. If a cluster of quarks and antiquarks satisfies $\mathcal{M}^2 - M_H^2 < \kappa^2$, the intermediate state sees the color confinement interaction. The meson LFWF connects the intermediate $q\bar{q}$ state, which is off of the P^- energy shell and thus off-the-invariant mass shell $\mathcal{M}^2 > m_H^2$ to the physical meson state with $\mathcal{M}^2 = m_H^2$. The LF angular momentum J^z is conserved at every vertex [43]

order 10^{120} times larger than what is observed if one computes the effects of quantum loops from QED. Similarly, QCD instantons and condensates in the instant-form vacuum give a contribution of order 10^{42}. The contribution of the Higgs VEV computed in the instant form vacuum is 10^{54} times too large.

In contrast, the vacuum in LF Hamlitonian theory is defined as the eigenstate of H_{LF} with lowest invariant mass. It is defined at fixed LF time τ within the causal horizon, and it is frame-independent; i.e., it is independent of the observer's motion. Vacuum loop diagrams from quantum field theory do not appear in the front-form vacuum since the + momenta are positive: $k_i^+ = k_i^0 + k_i^z \geq 0$, and the sum of + momenta is conserved at every vertex. The creation of particles cannot arise from the LF vacuum since $\sum_i k^{+i} \neq P^+_{vacuum} = 0$. Since propagation with negative k^+ does not appear, the LF vacuum is trivial up to possible $k^+ = 0$ "zero" modes. The physics associated with quark and gluon QCD vacuum condensates of the instant form are replaced by physical effects contained within the hadronic LFWFs in the hadronic domain. This is referred to as "in-hadron" condensates [47, 48, 49]. In the case of the Higgs theory, the traditional Higgs vacuum expectation value (VEV) is replaced by a "zero mode", analogous to a classical Stark or Zeeman field [50]. The Higgs LF zero mode [50] has no energy-momentum density, so it also gives zero contribution to the cosmological constant.

The universe is observed within the causal horizon, not at a single instant of time. The causal, frame-independent light-front vacuum can thus provide a viable match to the empty visible universe [49]. The huge contributions to the cosmological constant thus do not appear if one notes that the causal, frame-independent light-front vacuum has no quantum fluctuations – in dramatic contrast to to the acausal, frame-dependent instant-form vacuum; the cosmological constant arising from quantum field theory thus vanishes if one uses the front form. The observed nonzero value could could be a property of gravity itself, such as the "emergent gravity" postulated by E. Verlinde [51]. It is also possible that if one solves electroweak theory in a curved universe, the Higgs LF zero mode would be replaced with a field of nonzero curvature which could give a nonzero contribution to the cosmological constant.

7 The QCD Coupling at all Scales

The QCD running coupling $\alpha_s(Q^2)$ sets the strength of the interactions of quarks and gluons as a function of the momentum transfer Q. The dependence of the coupling Q^2 is needed to describe hadronic interactions at both long and short distances. The

QCD running coupling can be defined [52] at all momentum scales from a perturbatively calculable observable, such as the coupling $\alpha^s_{g_1}(Q^2)$, which is defined from measurements of the Bjorken sum rule. At high momentum transfer, such "effective charges" satisfy asymptotic freedom, obey the usual pQCD renormalization group equations, and can be related to each other without scale ambiguity by commensurate scale relations [53].

The dilaton $e^{+\kappa^2 z^2}$ soft-wall modification of the AdS_5 metric, together with LF holography, predicts the functional behavior of the running coupling in the small Q^2 domain [54]: $\alpha^s_{g_1}(Q^2) = \pi e^{-Q^2/4\kappa^2}$. Measurements of $\alpha^s_{g_1}(Q^2)$ are remarkably consistent [55] with this predicted Gaussian form; the best fit gives $\kappa = 0.513 \pm 0.007\ GeV$. See Fig. 10 Deur, de Teramond, and I [54, 56, 57] have also shown how the parameter κ, which determines the mass scale of hadrons and Regge slopes in the zero quark mass limit, can be connected to the mass scale Λ_s controlling the evolution of the perturbative QCD coupling. The high momentum transfer dependence of the coupling $\alpha_{g1}(Q^2)$ is predicted by pQCD. The matching of the high and low momentum transfer regimes of $\alpha_{g1}(Q^2)$ – both its value and its slope – then determines a scale $Q_0 = 0.87 \pm 0.08$ GeV which sets the interface between perturbative and nonperturbative hadron dynamics. This connection can be done for any choice of renormalization scheme, such as the $\overline{MS}$ scheme, as seen in Fig. 10. The result of this perturbative/nonperturbative matching is an effective QCD coupling defined at all momenta. The predicted value of $\Lambda_{\overline{MS}} = 0.339 \pm 0.019\ GeV$ from this analysis agrees well the measured value [58] $\Lambda_{\overline{MS}} = 0.332 \pm 0.019\ GeV$. These results, combined with the AdS/QCD superconformal predictions for hadron spectroscopy, allow us to compute hadron masses in terms of $\Lambda_{\overline{MS}}$: $m_p = \sqrt{2}\kappa = 3.21\ \Lambda_{\overline{MS}}$, $m_\rho = \kappa = 2.2\ \Lambda_{\overline{MS}}$, and $m_p = \sqrt{2} m_\rho$, meeting a challenge proposed by Zee [59]. The value of Q_0 can be used to set the factorization scale for DGLAP evolution of hadronic structure functions and the ERBL evolution of distribution amplitudes. Deur, de Téramond, and I have also computed the dependence of Q_0 on the choice of the effective charge used to define the running coupling and the renormalization scheme used to compute its behavior in the perturbative regime. The use of the scale Q_0 to resolve the factorization scale uncertainty in structure functions and fragmentation functions, in combination with the scheme-indepedent *principle of maximum conformality* (PMC) [60] for setting renormalization scales, can greatly improve the precision of pQCD predictions for collider phenomenology.

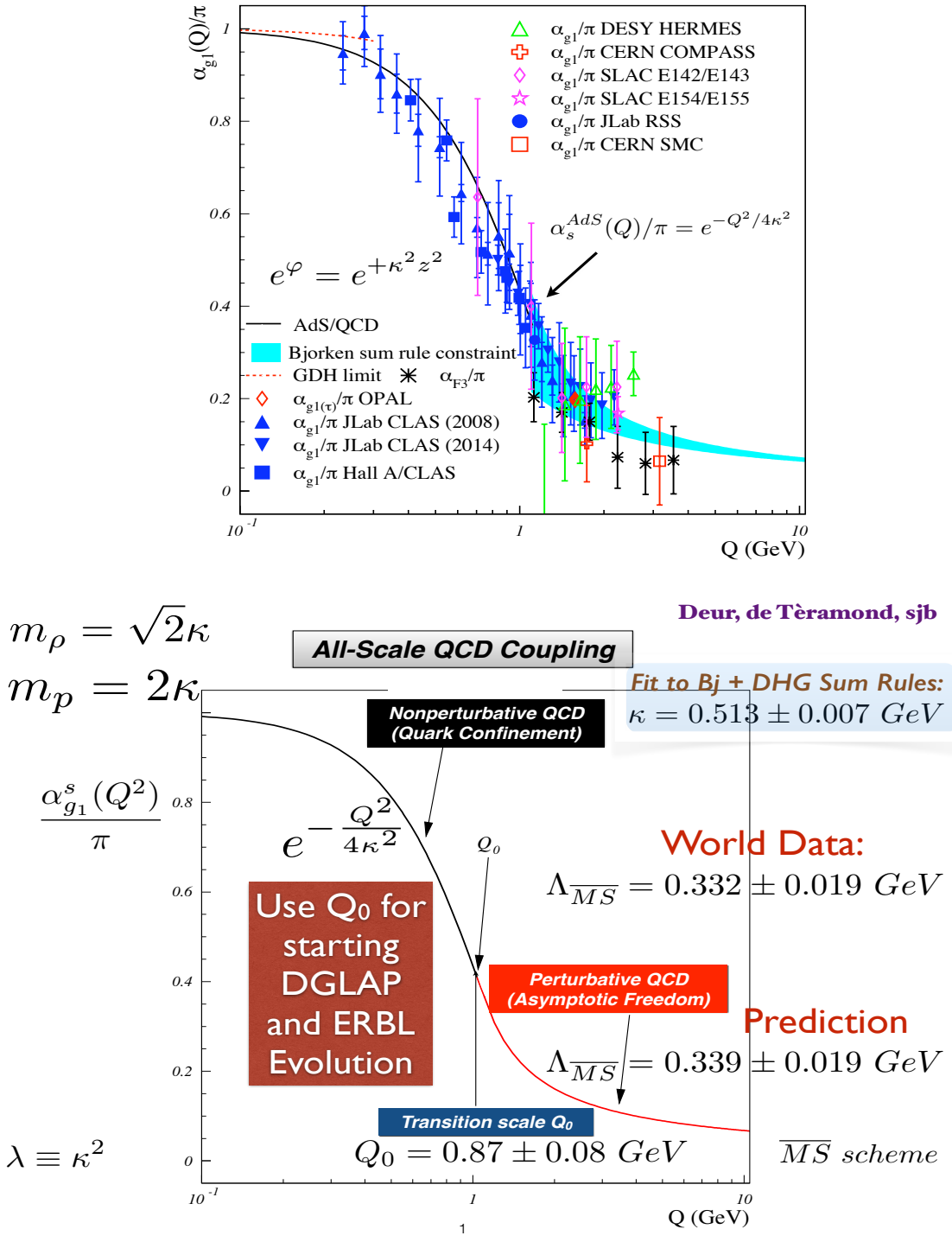

Figure 10: (A) Comparison of the predicted nonpertubative coupling, based on the dilaton $\exp(+\kappa^2 z^2)$ modification of the AdS_5 metric, with measurements of the effective charge $\alpha^s_{g_1}(Q^2)$, as defined from the Bjorken sum rule. (B) Prediction from LF Holography and pQCD for the QCD running coupling $\alpha^s_{g_1}(Q^2)$ at all scales. The magnitude and derivative of the perturbative and nonperturbative coupling are matched at the scale Q_0. This matching connects the perturbative scale $\Lambda_{\overline{MS}}$ to the nonpertubative scale κ which underlies the hadron mass scale. See Ref. [57].

8 Is the Momentum Sum Rule Valid for Nuclear Structure Functions?

Sum rules for deep inelastic scattering are usually analyzed using the operator product expansion of the forward virtual Compton amplitude, assuming it depends in the limit $Q^2 \to \infty$ on matrix elements of local operators such as the energy-momentum tensor. The moments of structure functions and other distributions can then be evaluated as overlaps of the target hadron's light-front wavefunction, as in the Drell-Yan-West formulae for hadronic form factors [61, 62, 63, 64]. The real phase of the resulting DIS amplitude and its OPE matrix elements reflects the real phase of the stable target hadron's wavefunction.

The "handbag" approximation to deeply virtual Compton scattering also defines the "static" contribution [65, 66] to the measured parton distribution functions (PDF), transverse momentum distributions, etc. The resulting momentum, spin and other sum rules reflect the properties of the hadron's light-front wavefunction. However, final-state interactions which occur *after* the lepton scatters on the quark, can give non-trivial contributions to deep inelastic scattering processes at leading twist and thus survive at high Q^2 and high $W^2 = (q+p)^2$. For example, the pseudo-T-odd Sivers effect [67] is directly sensitive to the rescattering of the struck quark. Similarly, diffractive deep inelastic scattering (DDIS) involves the exchange of a gluon after the quark has been struck by the lepton [68]. In each case the corresponding DVCS amplitude is not given by the handbag diagram since interactions between the two currents are essential. These "lensing" corrections survive when both W^2 and Q^2 are large since the vector gluon couplings grow with energy. Part of the final state phase can be associated with a Wilson line as an augmented LFWF [69] which does not affect the moments.

The Glauber propagation of the vector system V produced by the DDIS interaction on the nuclear front face and its subsequent inelastic interaction with the nucleons in the nuclear interior $V + N_b \to X$ occurs after the lepton interacts with the struck quark. The corresponding DVCS amplitude is not given by the handbag diagram since interactions between the two currents are essential. Because of the rescattering dynamics, the DDIS amplitude acquires a complex phase from Pomeron and Regge exchange; thus final-state rescattering corrections lead to nontrivial "dynamical" contributions to the measured PDFs; i.e., they are a consequence of the scattering process itself [70]. The $I = 1$ Reggeon contribution to DDIS on the front-face nucleon then leads to flavor-dependent antishadowing [71, 72]. This could explain why the NuTeV charged current measurement

$\mu A \to \nu X$ scattering does not appear to show antishadowing, in contrast to deep inelastic electron-nucleus scattering as discussed in Ref. [73].

Diffractive deep inelastic scattering is leading-twist. and it is an essential component of the two-step amplitude which causes shadowing and antishadowing of the nuclear PDF. It is important to analyze whether the momentum and other sum rules derived from the OPE expansion in terms of local operators remain valid when these dynamical rescattering corrections to the nuclear PDF are included. The OPE is derived assuming that the LF time separation between the virtual photons in the forward virtual Compton amplitude $\gamma^* A \to \gamma^* A$ scales as $1/Q^2$. However, the propagation of the vector system V produced by the DDIS interaction on the front face and its inelastic interaction with the nucleons in the nuclear interior $V + N_b \to X$ are characterized by a non-vanishing LF time interval in the nuclear rest frame. Note also that shadowing in deep inelastic lepton scattering on a nucleus involves nucleons facing the incoming lepton beam. The geometrical orientation of the shadowed nucleons is not a property of the the nuclear LFWFs used to evaluate the matrix elements of local currents. Thus leading-twist shadowing and antishadowing appear to invalidate the sum rules for nuclear PDFs. The same complications occur in the leading-twist analysis of deeply virtual Compton scattering $\gamma^* A \to \gamma^* A$ on a nuclear target. Thus the leading-twist multi-nucleon processes which produce shadowing and antishadowing in a nucleus are not accounted for using the $Q^2 \to \infty$ OPE analysis.

9 Summary

Light-Front Quantization provides a physical, frame-independent formalism for hadron dynamics and structure. Observables such as structure functions, transverse momentum distributions, and distribution amplitudes are defined from the hadronic light-front wavefunctions. One obtains new insights into the hadronic spectrum, light-front wavefunctions, and the $e^{-\frac{Q^2}{4\kappa^2}}$ Gaussian functional form of the QCD running coupling in the nonperturbative domain using light-front holography – the duality between the front form and AdS_5, the space of isometries of the conformal group.

In addition, superconformal algebra leads to remarkable supersymmetric relations between mesons and baryons of the same parity. The mass scale κ underlying confinement and hadron masses can be connected to the parameter $\Lambda_{\overline{MS}}$ in the QCD running coupling by matching the nonperturbative dynamics, as described by the effective conformal theory mapped to the light-front and its embedding in AdS space, to the pertur-

bative QCD regime. The result is an effective coupling defined at all momenta. This matching of the high and low momentum transfer regimes determines a scale Q_0 which sets the interface between perturbative and nonperturbative hadron dynamics. The use of Q_0 to resolve the factorization scale uncertainty for structure functions and distribution amplitudes, in combination with the principle of maximal conformality (PMC) for setting the renormalization scales [60], can greatly improve the precision of perturbative QCD predictions for collider phenomenology. The absence of vacuum excitations of the causal, frame-independent front form vacuum has important consequences for the cosmological constant. I have also discussed evidence that the antishadowing of nuclear structure functions is non-universal; *i.e.*, flavor dependent, and why shadowing and antishadowing phenomena may be incompatible with sum rules for nuclear parton distribution functions.

Acknowledgments

Presented at Tomsk National University, June 7, 2016. The results presented here are based on collaborations and discussions with Kelly Chiu, Alexandre Deur, Guy de Téramond, Guenter Dosch, Susan Gardner, Fred Goldhaber, Paul Hoyer, Dae Sung Hwang, Rich Lebed, Simonetta Liuti, Cedric Lorce, Valery Lyubovitskij, Matin Mojaza, Michael Peskin, Craig Roberts, Robert Shrock, Ivan Schmidt, Peter Tandy, and Xing-Gang Wu. This research was supported by the Department of Energy, contract DE–AC02–76SF00515. SLAC-PUB-XXXXX

References

[1] G. F. de Teramond, H. G. Dosch and S. J. Brodsky, Phys. Rev. D **91**, no. 4, 045040 (2015) doi:10.1103/PhysRevD.91.045040 [arXiv:1411.5243 [hep-ph]].

[2] H. G. Dosch, G. F. de Teramond and S. J. Brodsky, Phys. Rev. D **91**, no. 8, 085016 (2015) doi:10.1103/PhysRevD.91.085016 [arXiv:1501.00959 [hep-th]].

[3] V. de Alfaro, S. Fubini and G. Furlan, Nuovo Cim. A **34**, 569 (1976).

[4] S. J. Brodsky, G. F. De Teramond and H. G. Dosch, Phys. Lett. B **729**, 3 (2014) doi:10.1016/j.physletb.2013.12.044 [arXiv:1302.4105 [hep-th]].

[5] R. Haag, J. T. Lopuszanski and M. Sohnius, Nucl. Phys. B **88**, 257 (1975). doi:10.1016/0550-3213(75)90279-5

[6] S. Fubini and E. Rabinovici, Nucl. Phys. B **245**, 17 (1984). doi:10.1016/0550-3213(84)90422-X

[7] P. A. M. Dirac, Rev. Mod. Phys. **21**, 392 (1949). doi:10.1103/RevModPhys.21.392

[8] H. G. Dosch, G. F. de Teramond and S. J. Brodsky, Phys. Rev. D **92**, no. 7, 074010 (2015) doi:10.1103/PhysRevD.92.074010 [arXiv:1504.05112 [hep-ph]].

[9] G. 't Hooft, hep-th/0408148.

[10] T. Liu and B. Q. Ma, Phys. Rev. D **92**, no. 9, 096003 (2015) doi:10.1103/PhysRevD.92.096003 [arXiv:1510.07783 [hep-ph]].

[11] H. G. Dosch, G. F. de Teramond and S. J. Brodsky, arXiv:1612.02370 [hep-ph].

[12] S. J. Brodsky, H. C. Pauli and S. S. Pinsky, Phys. Rept. **301**, 299 (1998) doi:10.1016/S0370-1573(97)00089-6 [hep-ph/9705477].

[13] J. Terrell, Phys. Rev. **116**, 1041 (1959). doi:10.1103/PhysRev.116.1041

[14] R. Penrose, Proc. Cambridge Phil. Soc. **55**, 137 (1959). doi:10.1017/S0305004100033776

[15] S. J. Brodsky, M. Diehl and D. S. Hwang, Nucl. Phys. B **596**, 99 (2001) doi:10.1016/S0550-3213(00)00695-7 [hep-ph/0009254].

[16] S. J. Brodsky, D. S. Hwang, B. Q. Ma and I. Schmidt, Nucl. Phys. B **593**, 311 (2001) doi:10.1016/S0550-3213(00)00626-X [hep-th/0003082].

[17] I. Y. Kobzarev and L. B. Okun, Zh. Eksp. Teor. Fiz. **43**, 1904 (1962) [Sov. Phys. JETP **16**, 1343 (1963)].

[18] O. V. Teryaev, hep-ph/9904376.

[19] S. J. Brodsky, F. G. Cao and G. F. de Teramond, Phys. Rev. D **84**, 075012 (2011) doi:10.1103/PhysRevD.84.075012 [arXiv:1105.3999 [hep-ph]].

[20] J. R. Forshaw and R. Sandapen, Phys. Rev. Lett. **109**, 081601 (2012) doi:10.1103/PhysRevLett.109.081601 [arXiv:1203.6088 [hep-ph]].

[21] G. F. de Teramond, H. G. Dosch and S. J. Brodsky, Phys. Rev. D **87**, no. 7, 075005 (2013) doi:10.1103/PhysRevD.87.075005 [arXiv:1301.1651 [hep-ph]].

[22] S. J. Brodsky, G. F. de Teramond, H. G. Dosch and J. Erlich, Phys. Rept. **584**, 1 (2015) doi:10.1016/j.physrep.2015.05.001 [arXiv:1407.8131 [hep-ph]].

[23] T. Gutsche, V. E. Lyubovitskij, I. Schmidt and A. Vega, Phys. Rev. D **91**, no. 11, 114001 (2015) doi:10.1103/PhysRevD.91.114001 [arXiv:1501.02738 [hep-ph]].

[24] T. Gutsche, V. E. Lyubovitskij and I. Schmidt, Phys. Rev. D **94**, no. 11, 116006 (2016) doi:10.1103/PhysRevD.94.116006 [arXiv:1607.04124 [hep-ph]].

[25] G. F. de Teramond and S. J. Brodsky, Phys. Rev. Lett. **102**, 081601 (2009) doi:10.1103/PhysRevLett.102.081601 [arXiv:0809.4899 [hep-ph]].

[26] A. V. Smirnov, V. A. Smirnov and M. Steinhauser, Phys. Rev. Lett. **104**, 112002 (2010) doi:10.1103/PhysRevLett.104.112002 [arXiv:0911.4742 [hep-ph]].

[27] D. Ashery, Nucl. Phys. Proc. Suppl. **90**, 67 (2000) [Nucl. Phys. Proc. Suppl. **108**, 321 (2002)] doi:10.1016/S0920-5632(00)00875-6, 10.1016/S0920-5632(02)01354-3 [hep-ex/0008036].

[28] V. N. Gribov and L. N. Lipatov, Sov. J. Nucl. Phys. **15**, 438 (1972) [Yad. Fiz. **15**, 781 (1972)].

[29] G. Altarelli and G. Parisi, Nucl. Phys. B **126**, 298 (1977). doi:10.1016/0550-3213(77)90384-4

[30] Y. L. Dokshitzer, Sov. Phys. JETP **46**, 641 (1977) [Zh. Eksp. Teor. Fiz. **73**, 1216 (1977)].

[31] G. P. Lepage and S. J. Brodsky, Phys. Lett. **87B**, 359 (1979). doi:10.1016/0370-2693(79)90554-9

[32] G. P. Lepage and S. J. Brodsky, Phys. Rev. D **22**, 2157 (1980). doi:10.1103/PhysRevD.22.2157

[33] A. V. Efremov and A. V. Radyushkin, Phys. Lett. **94B**, 245 (1980). doi:10.1016/0370-2693(80)90869-2

[34] A. V. Efremov and A. V. Radyushkin, Theor. Math. Phys. **42**, 97 (1980) [Teor. Mat. Fiz. **42**, 147 (1980)]. doi:10.1007/BF01032111

[35] S. J. Brodsky and S. Gardner, Phys. Rev. Lett. **116**, no. 1, 019101 (2016) doi:10.1103/PhysRevLett.116.019101 [arXiv:1504.00969 [hep-ph]].

[36] H. C. Pauli and S. J. Brodsky, Phys. Rev. D **32**, 1993 (1985). doi:10.1103/PhysRevD.32.1993

[37] K. Hornbostel, S. J. Brodsky and H. C. Pauli, Phys. Rev. D **41**, 3814 (1990). doi:10.1103/PhysRevD.41.3814

[38] J. P. Vary, X. Zhao, A. Ilderton, H. Honkanen, P. Maris and S. J. Brodsky, Nucl. Phys. Proc. Suppl. **251-252**, 10 (2014) doi:10.1016/j.nuclphysbps.2014.04.002 [arXiv:1406.1838 [nucl-th]].

[39] S. J. Brodsky *et al.*, arXiv:1502.05728 [hep-ph].

[40] S. J. Brodsky and R. F. Lebed, Phys. Rev. Lett. **102**, 213401 (2009) doi:10.1103/PhysRevLett.102.213401 [arXiv:0904.2225 [hep-ph]].

[41] A. Banburski and P. Schuster, Phys. Rev. D **86**, 093007 (2012) doi:10.1103/PhysRevD.86.093007 [arXiv:1206.3961 [hep-ph]].

[42] C. Cruz-Santiago, P. Kotko and A. M. Sta?to, Prog. Part. Nucl. Phys. **85**, 82 (2015). doi:10.1016/j.ppnp.2015.07.002

[43] K. Chiu and S. J. Brodsky, SLAC-PUB-16904 (in preparation).

[44] S. J. Brodsky, R. Roskies and R. Suaya, Phys. Rev. D **8**, 4574 (1973). doi:10.1103/PhysRevD.8.4574

[45] S. J. Brodsky and G. F. de Teramond, arXiv:0901.0770 [hep-ph].

[46] A. Zee, Mod. Phys. Lett. A **23**, 1336 (2008). doi:10.1142/S0217732308027709

[47] A. Casher and L. Susskind, Phys. Rev. D **9**, 436 (1974). doi:10.1103/PhysRevD.9.436

[48] S. J. Brodsky and R. Shrock, Proc. Nat. Acad. Sci. **108**, 45 (2011) doi:10.1073/pnas.1010113107 [arXiv:0905.1151 [hep-th]].

[49] S. J. Brodsky, C. D. Roberts, R. Shrock and P. C. Tandy, Phys. Rev. C **82**, 022201 (2010) doi:10.1103/PhysRevC.82.022201 [arXiv:1005.4610 [nucl-th]].

[50] P. P. Srivastava and S. J. Brodsky, Phys. Rev. D **66**, 045019 (2002) doi:10.1103/PhysRevD.66.045019 [hep-ph/0202141].

[51] E. P. Verlinde, arXiv:1611.02269 [hep-th].

[52] G. Grunberg, Phys. Lett. **95B**, 70 (1980) Erratum: [Phys. Lett. **110B**, 501 (1982)]. doi:10.1016/0370-2693(80)90402-5

[53] S. J. Brodsky and H. J. Lu, Phys. Rev. D **51**, 3652 (1995) doi:10.1103/PhysRevD.51.3652 [hep-ph/9405218].

[54] S. J. Brodsky, G. F. de Teramond and A. Deur, Phys. Rev. D **81**, 096010 (2010) doi:10.1103/PhysRevD.81.096010 [arXiv:1002.3948 [hep-ph]].

[55] A. Deur, V. Burkert, J. P. Chen and W. Korsch, Phys. Lett. B **650**, 244 (2007) doi:10.1016/j.physletb.2007.05.015 [hep-ph/0509113].

[56] A. Deur, S. J. Brodsky and G. F. de Teramond, Phys. Lett. B **750**, 528 (2015) doi:10.1016/j.physletb.2015.09.063 [arXiv:1409.5488 [hep-ph]].

[57] S. J. Brodsky, G. F. de Teramond, A. Deur and H. G. Dosch, Few Body Syst. **56**, no. 6-9, 621 (2015) doi:10.1007/s00601-015-0964-1 [arXiv:1410.0425 [hep-ph]].

[58] K. A. Olive *et al.* [Particle Data Group], Chin. Phys. C **38**, 090001 (2014). doi:10.1088/1674-1137/38/9/090001

[59] A. Zee, Princeton, UK: Princeton Univ. Pr. (2010) 576 p

[60] M. Mojaza, S. J. Brodsky and X. G. Wu, Phys. Rev. Lett. **110**, 192001 (2013) doi:10.1103/PhysRevLett.110.192001 [arXiv:1212.0049 [hep-ph]].

[61] S. J. Brodsky and S. D. Drell, Phys. Rev. D **22**, 2236 (1980). doi:10.1103/PhysRevD.22.2236

[62] S. Liuti, A. Rajan, A. Courtoy, G. R. Goldstein and J. O. Gonzalez Hernandez, Int. J. Mod. Phys. Conf. Ser. **25**, 1460009 (2014) doi:10.1142/S201019451460009X [arXiv:1309.7029 [hep-ph]].

[63] C. Mondal and D. Chakrabarti, Eur. Phys. J. C **75**, no. 6, 261 (2015) doi:10.1140/epjc/s10052-015-3486-6 [arXiv:1501.05489 [hep-ph]].

[64] C. Lorce, B. Pasquini and M. Vanderhaeghen, JHEP **1105**, 041 (2011) doi:10.1007/JHEP05(2011)041 [arXiv:1102.4704 [hep-ph]].

[65] S. J. Brodsky, AIP Conf. Proc. **1105**, 315 (2009) doi:10.1063/1.3122202 [arXiv:0811.0875 [hep-ph]].

[66] S. J. Brodsky, Nucl. Phys. A **827**, 327C (2009) doi:10.1016/j.nuclphysa.2009.05.068 [arXiv:0901.0781 [hep-ph]].

[67] S. J. Brodsky, D. S. Hwang and I. Schmidt, Phys. Lett. B **530**, 99 (2002) doi:10.1016/S0370-2693(02)01320-5 [hep-ph/0201296].

[68] S. J. Brodsky, P. Hoyer, N. Marchal, S. Peigne and F. Sannino, Phys. Rev. D **65**, 114025 (2002) doi:10.1103/PhysRevD.65.114025 [hep-ph/0104291].

[69] S. J. Brodsky, B. Pasquini, B. W. Xiao and F. Yuan, Phys. Lett. B **687**, 327 (2010) doi:10.1016/j.physletb.2010.03.049 [arXiv:1001.1163 [hep-ph]].

[70] S. J. Brodsky, D. S. Hwang, Y. V. Kovchegov, I. Schmidt and M. D. Sievert, Phys. Rev. D **88**, no. 1, 014032 (2013) doi:10.1103/PhysRevD.88.014032 [arXiv:1304.5237 [hep-ph]].

[71] S. J. Brodsky and H. J. Lu, Phys. Rev. Lett. **64**, 1342 (1990). doi:10.1103/PhysRevLett.64.1342

[72] S. J. Brodsky, I. Schmidt and J. J. Yang, Phys. Rev. D **70**, 116003 (2004) doi:10.1103/PhysRevD.70.116003 [hep-ph/0409279].

[73] I. Schienbein, J. Y. Yu, C. Keppel, J. G. Morfin, F. Olness and J. F. Owens, Phys. Rev. D **77**, 054013 (2008) doi:10.1103/PhysRevD.77.054013 [arXiv:0710.4897 [hep-ph]].